

WATERSPOUT STUDIES II - GROUND AND CLOUD EFFECTS

G.L. ROFF and B.R. MORTON

Centre for Dynamical Meteorology
Department of Mathematics, Monash University
Clayton, VIC 3168, AUSTRALIA

Intense geophysical columnar vortices are classified as tornadoes, waterspouts, dust devils or fire whirls depending on the prevailing environmental circumstances. Such distinction is not always obvious (Forbes and Wakimoto, 1983), with waterspouts that form over sea able to move onto land while tornadoes and dust devils that form over land can move out to sea (Dinwiddie, 1959; Golden, 1968, 1971, 1974; Golden and Purcell, 1978; Elsom, 1988). However all vortices require a source of forcing to concentrate the local vorticity, and this source can be used to distinguish the more intense and longer lived tornadoes and waterspouts. These vortices obtain their forcing from the vertical wind field of an associated parent cloud, whereas the forcing for the weaker dust devils and fire whirls comes from strong surface heating.

Apart from the forcing source and the intensity of the resulting vortex, these geophysical vortices have similar lifecycles and all vortices, whether natural or laboratory generated, are similar near their cores (Fiedler and Rotunno, 1986). This similarity has allowed the successful laboratory modelling of the geophysical vortices (Maxworthy, 1982) and also successful numerical simulation. Our paper compares results from a numerical simulation of the Great Salt Lake waterspout observed on 26 June 1985 (Simpson et al, 1991) with reported laboratory vortex phenomena including one- and two-cell vortices, vortex breakdown and centrifugal waves (Snow, 1982).

1. INTRODUCTION

Vortices range from narrow and laminar, with strong axial updrafts, to broad and turbulent, with weak updrafts. These two types occur often as one- or two-cell vortices (Figure 1)¹, respectively, where the former are supercritical, unable to sustain centrifugal (inertial) waves with strong axial upflow, and the latter are subcritical, able to sustain such waves, and having axial downflow surrounded by annular upflow (Fiedler and Rotunno, 1986).

Generally a vortex starts as a one-cell and may remain such or convert to a two-cell structure as a "vortex breakdown" forms aloft and moves down the axis (upstream), with complete conversion when this breakdown reaches the lower surface (Figure 1c). Such axisymmetric vortex breakdowns (Figure 1a) are generally characterized by an axial stagnation point with flow reversal downstream enclosed in a swollen stream surface (Faler and Leibovich, 1977). Flow behaviour in a concentrated vortex may be characterized by the swirl parameter $Sm = |V|/W$, where V and W are the maximum azimuthal and updraft velocities respectively, evaluated over

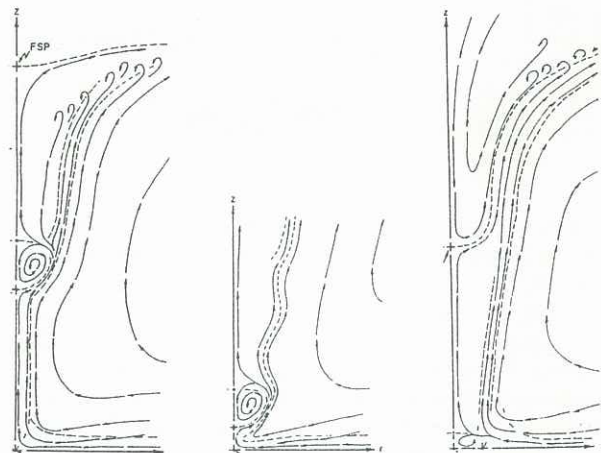


Figure 1: Schematic of (a) a low-swirl one-cell vortex suffering vortex breakdown, (b) a "drowned vortex jump", and (c) an intermediate-swirl two-cell vortex (Reproduced from Snow, 1982).

the whole vortex domain. Vortices can suffer such breakdowns only when subcritical, with Sm greater or equal to a critical value, which has been measured as ≈ 0.84 (Lugt, 1989).

Vortex breakdown is hard to observe in nature due to masking by dust, spray, the condensation funnel or parent cloud, but axial stagnation points in pendant funnels support their existence and actual vortex breakdowns have been observed (Hoecker, 1960; Golden and Purcell, 1977).

The numerical simulations of the Great Salt Lake waterspout observed on 26 June 1985 (Simpson et al, 1991), discussed in the previous paper, will be used here to study the formation of one- and two-cell vortices, vortex breakdown and vortex decay from both cloud and surface effects. Since all the simulated one-cell vortices behaved similarly, we concentrate on those which formed when the vortex model was embedded at the anticyclonic centre within the LINE cloud model output at 28min into cloud evolution. At this time there are strong updrafts and circulations present and we shall consider both time constant (TC) and time varying (TV) boundary conditions (A28L TC and A28L TV, respectively). We shall take as representative of the two-cell structure the vortex formed when embedded using time varying boundary conditions within the LINE cloud model output at 20min cloud time and constrained to follow the anticyclonic centre (case A20MC).

¹Reproduced from Snow, 1982

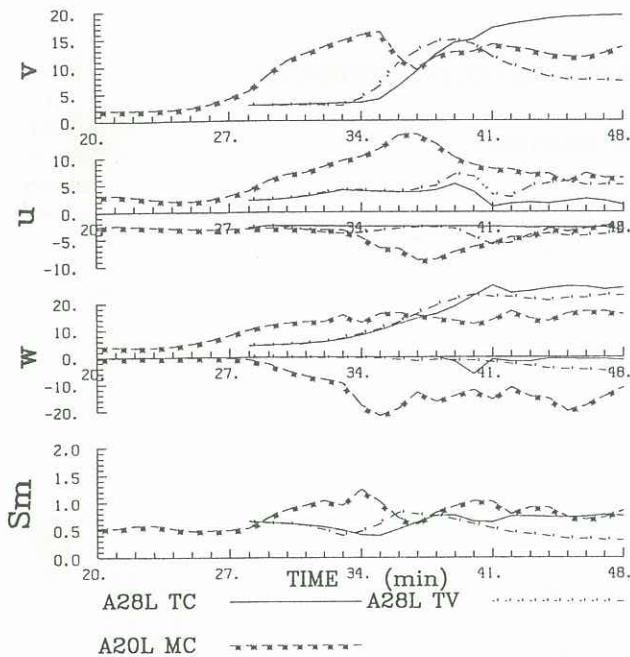


Figure 2: Plots, against vortex model time in minutes, of the maximum values of the absolute azimuthal velocity (V), the maximum and minimum values of the radial (U) and vertical (W) velocities, in ms^{-1} , and the modified swirl parameter (Sm) values found in the inner cylindrical domain for vortex model runs centered at the anticyclonic center (at 1200m elevation AGL) in the LINE cloud model starting at 28min cloud model time with fixed (A28L TC) and varying (A28L TV) boundary data. Also plots for the time varying anticyclonic moving center run started at 20min cloud model time (A20MC) are given.

2. VORTEX DECAY: GROUND EFFECTS

The vortex initiated at 28min at the LINE anticyclonic centre using fixed boundary conditions (A28L TC) was one-cell and showed no sign of decay during the 20min, run as seen by the constantly increasing maximum values of its azimuthal and vertical velocity fields (Figure 2). This is unlike the observed Great Salt Lake waterspout lifetime of 5min (Simpson et al, 1991) but is typical of vortex models which use constant boundary conditions (Howells and Smith, 1983). The TC vortex intensification can be explained as the model was started when the cloud had high circulation and strong updrafts and these conditions are maintained using the fixed boundary conditions used.

The swirl parameter for this run remained below the critical .84 (Figure 2). While the vortex did not display any sign of a breakdown descending from aloft, Sm approached the critical value after 9min into the run. as the maximum radial inflow in a jet near the surface, overshoot the axis causing a surface vortex breakdown and centrifugal (inertial) waves or Bodewadt instabilities (Proctor, 1982) to travel up the axis within the core. These inertial waves were seen as oscillations in the radial and vertical velocity fields on the axis, and the surface vortex breakdown as a strong axial downdraft near the surface (Figure 3). Neither phenomena disrupted the vortex intensification. The maximum azimuthal velocity and largest pressure deficit occurred near the vortex breakdown and these features were similar to those observed in the laboratory "drowned vortex jump" (Figure 1b).

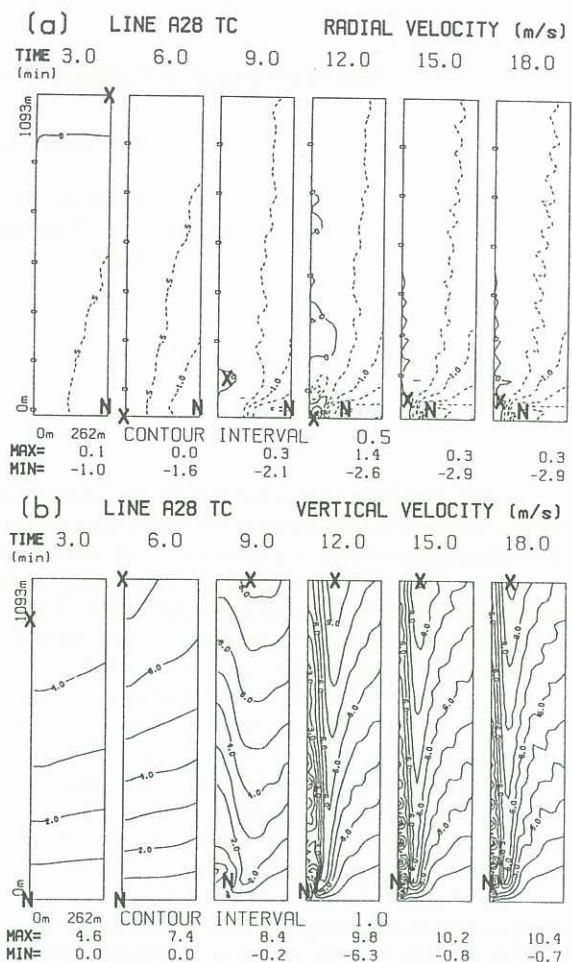


Figure 3: Three minute time series solution contours over the inner corner domain (radius 262m, height 1093m) from 3min to 18min vortex time for the fixed boundary condition 20min A28L TC run showing the (a) radial and (b) vertical velocity fields (ms^{-1}).

When the vortex boundary conditions are allowed to evolve with the cloud (A28L TV), a more realistic growth and decay cycle may be observed (Figure 2). Initially the one-cell vortex evolves as in the A28L TC case developing stronger rotation and as Sm approaches the critical value, forming a surface vortex breakdown and axial Bodewadt instabilities (Figure 4). However, at this stage the model cloud begins to decay, developing downdrafts near the vortex site which cut off moist low level inflow to the model vortex domain. Unlike the fixed boundary condition run (A28L TC) the variable boundary conditions allow the vortex model to react by cutting off the radial inflow that feeds the surface jet. This prevents high-spin air from reaching the core, causing the vortex to decrease in strength near the surface and the surface breakdown and inertial waves to decay. The decay process, seen as a loss of core structure in the radial and vertical velocity fields (Figure 4), moves up the axis along with the maximum azimuthal velocity and lowest axial pressure deficit while the Sm values decrease (Figure 2), indicating the cessation of axial wave activity.

The time varying boundary conditions form the drowned vortex jump, as in the fixed boundary condition run, but create a more realistic waterspout simulation by allowing the cloud to initialize the vortex and then lead to its decay. Observed wa-

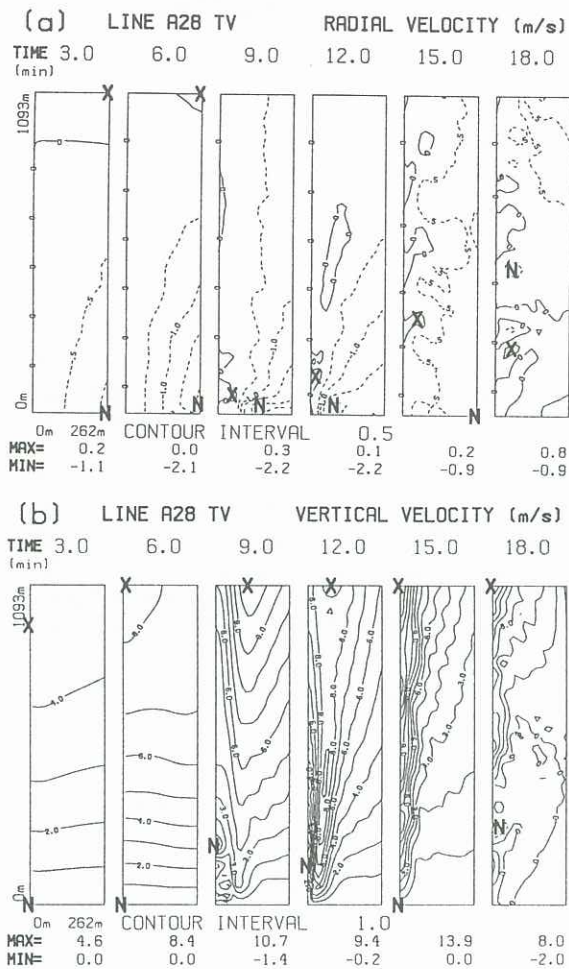


Figure 4: Three minute time series solution contours over the inner corner domain (radius 262m, height 1093m) from 3min to 18min vortex time for the 20min A28L TV run showing the (a) radial, and (b) vertical velocity fields (ms^{-1}).

terspouts often decay in a similar manner when gust fronts cut the vortex off from the surface (Golden, 1974b; Lilly, 1982).

3. VORTEX DECAY: CLOUD EFFECTS

As in the previous runs, the A20MC vortex which used variable boundary conditions and followed the clouds anticyclonic centre started as a one-cell vortex and developed an axial surface vortex breakdown and Bodewadt instabilities at 9min as S_m approached the critical value (Figure 2). Again these instabilities have little effect on the vortex development although in this case a secondary vortex breakdown now develops aloft (2500m) and prevents the tight axial core from growing up the axis (Figure 5a). As the vortex core continues to spin up, this breakdown moves down the axis, broadening the core aloft and leaving an elongated flow reversal region behind it.

The extent of the secondary breakdown along the axis is seen in the radial and vertical velocity fields near the corner (Figure 6), and at 15min vortex time the situation is similar to the intermediate-swirl vortex (Figure 1c), with leading breakdown near the surface, secondary breakdown aloft and large axial downflow above this. The inertial waves are trapped between these two breakdowns and a complete two-cell vortex forms as the secondary breakdown approaches the surface.

The maximum azimuthal velocity and largest pressure deficit are always associated with the first breakdown, except near 18min vortex time. This departure is not due to surface effects like the A28L TV run, as the cloud continues to provide low-level radial inflow; rather it is due to cloud effects that cause the two-cells broad downflow core aloft to become unstable. The instability aloft is first indicated after 15min vortex time as a wave, seen in the full vortex domain radial and ver-

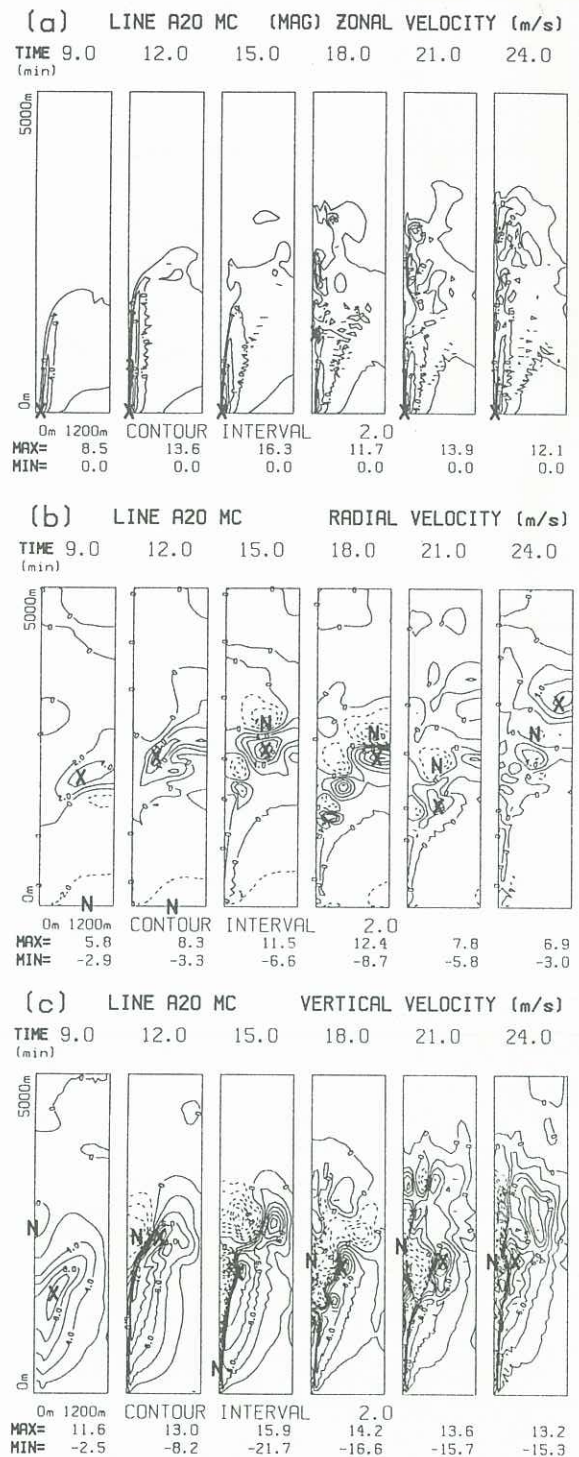


Figure 5: Three minute time series solution contours over the full vortex domain (radius 1200m, height 5000m) from 9min to 27min vortex time for the 28min A20MC run showing the (a) absolute zonal, (b) radial, and (c) vertical velocity fields (ms^{-1}).

tical velocity fields to be toroidal in nature (Figure 5), which is associated with large pressure signatures moving down the the core edge disrupting the upper vortex but not the lower region to the same extent.

This toroidal system forces the full length of the core to expand as it moves down the vortex, decreasing the maximum azimuthal velocity (Figure 2). At 18min the leading toroid progresses far enough down the core for its flow field to cause strong radial inflow to the axis. This inflow, and conservation of angular momentum, causes the maximum azimuthal velocity and largest pressure deficit to occur here (1250m) instead of at the first-breakdown at the surface. With these toroidal flow fields now reaching the axis, the core downflow is totally cut off from its parent cloud source and so diminishes. The surface radial inflow now begins to re-establish an axial upflow which attempts to regenerate the vortex. During this run Sm achieves the largest values of all runs, with a maximum of 1.2 well above the critical value, for extended periods and as is indicated by these Sm values is the only run to become two-cell.

The toroidal waves destroyed the vortex aloft while the lower levels lost intensity but remained intact. This vortex decay thus differs appreciably from the two previous runs but the toroids do resemble bulges that were observed travelling down the funnel in a video tape of the actual Great Salt Lake waterspout. Such downward travelling waves have been observed in other geophysical vortices (Hurd, 1950; Reber, 1954; Golden, 1974).

4. CONCLUSIONS

Axisymmetric numerical simulations of the Great Salt Lake waterspout event of 26 June 1985 have been compared with laboratory vortices and have exhibited important features of the latter. The numerical vortices with imposed time constant boundary conditions behaved in a like manner to the low-swirl one-cell laboratory vortices displaying vortex breakdown, drowned vortex jumps and inertial waves. When time varying boundary conditions were used, these features were also present but the cloud influenced vortex development more directly and more realistic vortex evolution was observed with decay as the cloud decayed.

The final simulation had time varying boundary conditions and was able to follow the anticyclonic centre of the cloud, produced a two-cell vortex that displayed decay from aloft due to the downward motion of toroidal waves which resembled those observed in the actual waterspout sighting.

REFERENCES

- Dinwiddie,FB (1959) Waterspout-Tornado structure and behavior at Nags Head, N.C., August 12, 1952. *Mon. Wea. Rev.*, **87**, 239-250.
- Elsom,D (1988) Catch a Falling Frog. *New Scientist*, **118**, 38-40.
- Faler,JH and Leibovich,S (1977) Disrupted states of vortex flow and vortex breakdown. *Phys.Fluids*, **20**, 1385-1400.
- Fiedler,BH and Rotunno,R (1986) A Theory for the Maximum Windspeeds in Tornado-like Vortices. *J.Atmos.Sci.*, **43**,2328-2340.
- Forbes,GS and Wakimoto,RM (1983) A concentrated outbreak of Tornadoes, Downbursts and Microbursts, and implications regarding Vortex classification. *Mon. Wea. Rev.*, **111**, 220-235.
- Golden,JH (1968) Waterspouts at Lower Matecumbe Key, Florida, September 2, 1967. *Weather*, **23**, 103-114.
- Golden,JH (1974) The Life Cycle of Florida Keys Waterspouts. *I. J. Atmos. Sci.*, **13**, 676-692.
- Golden,JH (1971) Waterspouts and tornadoes over south

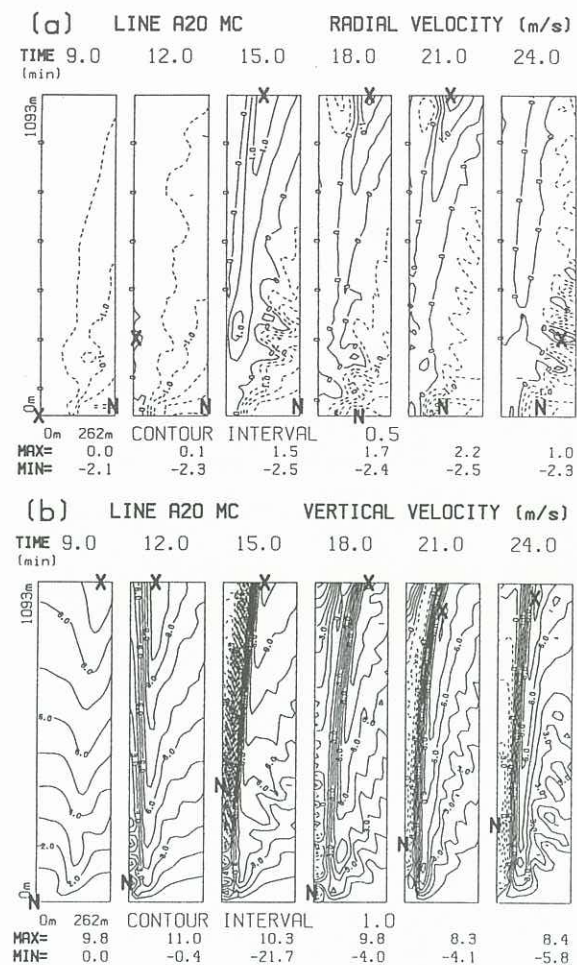


Figure 6: Three minute time series solution contours over the inner corner domain (radius 262m, height 1093m) from 9min to 24min vortex time for the 28min A20MC run showing the (a) radial, and (b) vertical velocity fields (ms^{-1}).

Florida. *Mon. Wea. Rev.*, **99**, 146-154.

Golden,JH and Purcell,D (1977) Photogrammetric velocities for the Great Bend, Kansas, Tornado of 30 August 1974: Accelerations and Asymmetries. *Mon.Weather Rev.*, **105**, 485-492.

Hoecker,WH (1960) Wind speed and air flow patterns in the Dallas tornado of April 2, 1957. *Mon. Wea. Rev.*, **88**, 167-180.

Howells,PAC and Smith,RK (1983) Numerical Simulations of Tornado-Like Vortices I: Vortex Evolution. *Geophys.Astrophys.Fluid Dyn.*, **27**, 253-284.

Hurd,WE (1950) Some Phases of Waterspot Behavior. *Weatherwise*, **3**, 75-82.

Lilly,DK (1982) The Development and Maintenance of Rotation in Convective Storms. *Intense Atmospheric Vortices*, Springer-Verlag, L.Bengtsson and J.Lighthill, eds., 149-160.

Lugt,HJ (1989) Vortex Breakdown in Atmospheric Columnar Vortices. *Bull.Amer.Meteor.Soc.*, **70**, 1526-1537.

Maxworthy,T (1982) The Laboratory Modelling of Atmospheric Vortices: A Critical Review. *Intense Atmospheric Vortices*, Springer-Verlag, L.Bengtsson and J.Lighthill, eds., 229-246.

Proctor,FH (1982) A numerical study on the evolution of Tornadoes. Ph.D, Texas A&M University.

Reber,CM (1954) The South Platte Valley Tornadoes of June 7, 1953. *Bull. Amer. Meteor. Soc.*, **35**, 191 - 197.

Simpson,J, Roff,GL, Morton,BR, Labas,K, Dietachmayer, D, McCumber,M and Penc,R (1991) A Great Salt Lake Waterspout. *Mon. Wea. Rev.*, **119**, 2741-2770.

Snow,JT (1982) A Review of Recent Advances in Tornado Vortex Dynamics. *Reviews of Geophysics and Space Physics*, **20**, 953-964.